Electrochemical and Solid-State Letters, **13** (4) A39-A42 (2010)
1099-0062/2010/13(4)/A39/4/$28.00 © The Electrochemical Society

Lithium Borate Cluster Salts as Redox Shuttles for Overcharge Protection of Lithium-Ion Cells

Zonghai Chen,[a,*,z] Jun Liu,[a] A. N. Jansen,[a,*] G. GirishKumar,[b] Bill Casteel,[b] and K. Amine[a,*,z]

[a]*Chemical Sciences and Engineering Division, Argonne National Laboratory, Argonne, Illinois 60439, USA*
[b]*Air Products and Chemicals Incorporated, Allentown, Pennsylvania 18195, USA*

Redox shuttle is a promising mechanism for intrinsic overcharge protection in lithium-ion cells and batteries. Two lithium borate cluster salts are reported to function as both the main salt for a nonaqueous electrolyte and the redox shuttle for overcharge protection. Lithium borate cluster salts with a tunable redox potential are promising candidates for overcharge protection for most positive electrodes in state-of-the-art lithium-ion cells.
 [DOI: 10.1149/1.3299251]

Manuscript submitted October 20, 2009; revised manuscript received November 13, 2009. Published February 1, 2010.

Because of life and safety issues with lithium-ion cells, they must be charged to a specific upper cutoff voltage, not beyond. Overcharge generally occurs when a charger forces current through a lithium-ion cell after the cell has already reached its upper cutoff voltage. Overcharging is very dangerous in lithium-ion cells or batteries. It can lead to chemical and electrochemical reactions among the battery components,[1,2] gas release, and rapid temperature elevation.[1-3] It can also trigger self-accelerating reactions and even explosions.[4] To prevent lithium-ion cells from overcharging, redox-shuttle electrolyte additives have long been pursued for overcharge protection.[5-17] The redox shuttle molecule (S) has a defined redox potential, at which it can be oxidized on the positive electrode and form a radical cation ($S^{\bullet+}$)

$$S \rightarrow S^{\bullet+} + e^- \quad [1]$$

The radical cation then travels to the negative electrode through the electrolyte and is reduced

$$S^{\bullet+} + e^- \rightarrow S \quad [2]$$

The redox shuttle molecule then diffuses back to the positive electrode for the next redox cycle. The electron transports from the positive electrode to the negative electrode through an external circuit, which is generally applied by a cell charger. During normal operation, the redox potential of the redox shuttle is not reached, and the redox shuttle molecules stay inactive. When the cell is overcharged, the potential of the positive electrode increases, and the redox cycle of the redox shuttle molecules is then activated. The net reaction is to shuttle the charge forced by the external circuit through the lithium-ion cell without further forcing intercalation/deintercalation of lithium in the cell.

The reported redox shuttle materials include ferrocene derivatives[5,6] for 3 V secondary batteries and substituted aromatic compounds[7-9,12-14] for 4 V lithium-ion batteries. According to Narayanan et al.,[18] the limiting shuttle current, I_{max}, that the redox shuttle can carry between two planar electrodes is given by

$$I_{max} = nFADC/L \quad [3]$$

where n is the number of elementary charge carried by the shuttle, F is Faraday's constant, A is the area of the planar electrodes, D is the diffusion coefficient of the shuttle, C is the concentration of the redox shuttle, and L is the distance between two planar electrodes. Both A and L are generally fixed by the geometry of the lithium-ion cells, and D is specified by the chemical and physical characteristics of the solvent and the redox shuttle. Therefore, the solubility of the redox shuttle plays a key role in determining the I_{max} of the redox system. However, the aromatic redox shuttles[14] have limited solubilities in nonaqueous solvents. Such redox shuttles are only suitable for some low rate applications, and their application for high rate and high power lithium-ion cells is still questionable.

An additional disadvantage of the above-mentioned redox shuttles is that these electrolyte additives generally stay inactive during normal operation of the lithium-ion cells. They are only activated during the overcharge condition, which is considered a rare event during the whole lifespan of the lithium-ion cell. Some cells might not even be subjected to overcharge abuse during their life. In this work, two redox shuttles, $Li_2B_{12}H_{12-x}F_x$ (x = 9 and 12), are introduced. It is shown that $Li_2B_{12}H_{12-x}F_x$ can act both as salts for nonaqueous electrolytes and as redox shuttles for the overcharge protection of lithium-ion cells.

Experimental

The two lithium borate cluster salts, $Li_2B_{12}H_{12-x}F_x$ (x = 9 and 12), were synthesized and provided by Air Products and Chemicals, Inc. and were used without further purification.

The positive electrode laminate consisted of 84 wt % $Li_{1.1}[Ni_{1/3}Co_{1/3}Mn_{1/3}]_{0.9}O_2$ (L333), 8 wt % carbon black (TB5500), and 8 wt % poly(vinylidene fluoride) (PVDF). The negative electrode laminate consisted of 90 wt % mesocarbon microbeads (MCMB-1028, D_{50} = 10 μm), 2 wt % vapor-grown carbon fiber, and 8 wt % PVDF.

The electrochemical performance of the lithium borate cluster salts was evaluated with 2032-type coin cells. The cell stack consisted of a negative electrode (MCMB), a microporous polypropylene separator (Celgard 3501), a positive electrode (L333), and an appropriate amount of electrolyte.

Cyclic voltammograms of the $Li_2B_{12}H_{12-x}F_x$-containing electrolyte were collected with a BAS-Zahner IM6 impedance analyzer and a Li/Li/Pt three-electrode cell. The diameter of the Pt working electrode was about 1 mm. Cyclic voltammetry was performed in an argon-filled glove box.

Results and Discussion

The redox shuttles tested in this work are lithium salts, which have very good solubility in a nonaqueous solvent and can be used as the main salts for nonaqueous electrolytes. Both $Li_2B_{12}H_3F_9$ and $Li_2B_{12}F_{12}$ can be easily dissolved in most commonly used carbonates of up to 0.5 M, which provides Li^+ concentration of up to 1.0 M. Figure 1 shows the conductivity of 0.4 M lithium borate cluster salts (x = 9 and 12) in 3:7 ethylene carbonate (EC)/ethyl methyl carbonate (EMC) as a function of reciprocal temperature. The conductivity of 1.2 M $LiPF_6$ in EC/EMC was also shown in Fig. 1 as a baseline. Because of the structural similarity between $Li_2B_{12}H_3F_9$ and $Li_2B_{12}F_{12}$, the electrolytes comprising the salts achieve almost the same conductivity at various temperatures. The conductivity of $Li_2B_{12}H_{12-x}F_x$ in this solvent system is about one-half the conductivity of $LiPF_6$-based electrolytes. It will be reported in the future that optimized electrolytes can meet the requirement for high power applications.

* Electrochemical Society Active Member.
z E-mail: Zonghai.chen@anl.gov; amine@cmt.anl.gov

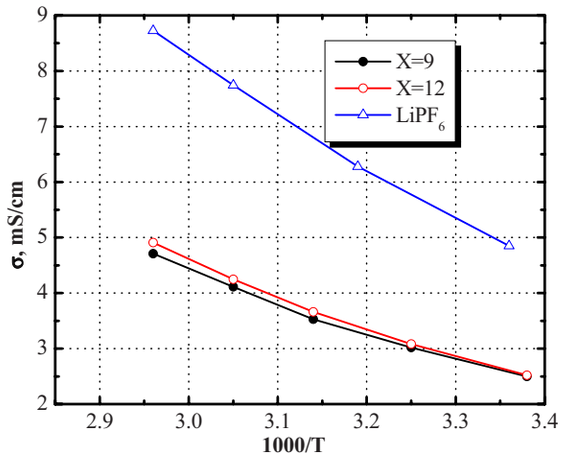

Figure 1. (Color online) Conductivity vs temperature of 0.4 M $Li_2B_{12}H_3F_9$, 0.4 M $Li_2B_{12}F_{12}$, and 1.2 M $LiPF_6$ in 3:7 EC/EMC.

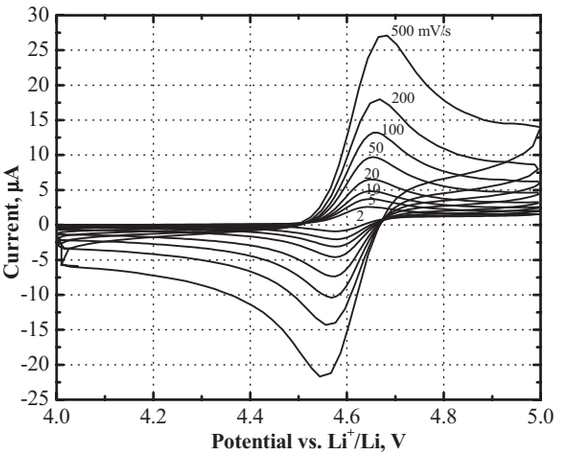

Figure 3. Cyclic voltammogram of 0.01 M $Li_2B_{12}F_{12}$ with different scanning rates. Background solution is 1.0 M $LiPF_6$ in 3:7 EC/EMC.

The most promising use of $Li_2B_{12}H_{12-x}F_x$ is not only as lithium salt for lithium-ion batteries but also as a redox shuttle for the overcharge protection. In lithium salts for nonaqueous electrolytes, such as $LiPF_6$, the anion is electrochemically stable within the working potential window. What distinguishes lithium borate cluster salts is that their anions, $B_{12}F_{12-x}H_x^{2-}$, can be reversibly oxidized and reduced at a higher potential than 4.2 V vs Li^+/Li. Therefore, the lithium borate cluster salts can work as both the main salt and the redox shuttle for state-of-the-art 4 V lithium-ion cells. Figure 2 shows cyclic voltammograms of 0.01 M $Li_2B_{12}F_{12-x}H_x$ (x = 9 and 12) salts. The background solution is 1.0 M $LiPF_6$ in 3:7 EC/EMC. As a control experiment, the cyclic voltammogram of the background solution (1.0 M $LiPF_6$ in 3:7 EC/EMC) was obtained for comparison and is given in Fig. 2a. Figure 2a clearly shows no major electrochemical reaction of the background solution in the voltage window from 4.0 to 4.8 V vs Li^+/Li. The small irreversible peak at 4.9 V vs Li^+/Li is probably due to the oxidation of the solvent, i.e., EC or EMC. Figure 2b clearly shows a reversible electrochemical reaction of $B_{12}F_9H_3^{2-}$ at about 4.5 V vs Li^+/Li. The potential difference between the anionic peak and the cathodic peak is about 100 mV (>69 mV), which suggests a single electron transfer reaction. Figure 2c shows that $B_{12}F_{12}^{2-}$ has a similar electrochemical reactivity, except that its redox potential is about 0.1 V higher than that of $B_{12}F_9H_3^{2-}$.

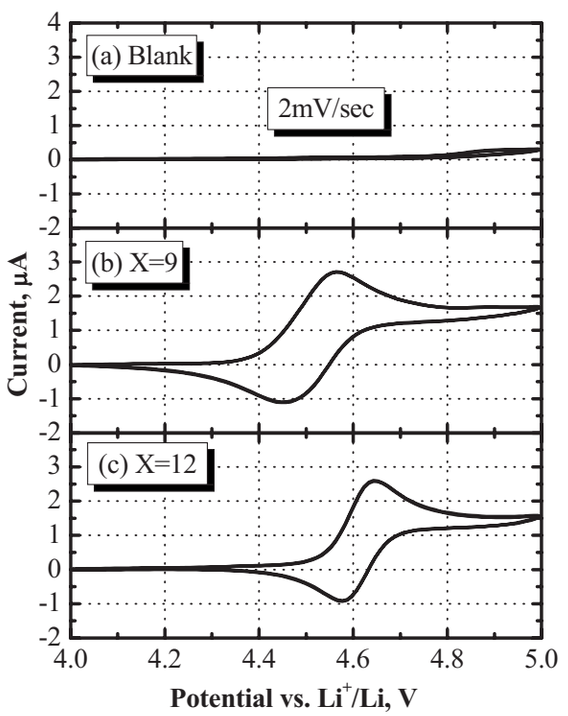

Figure 2. Cyclic voltammogram of (a) 1.0 M $LiPF_6$ in 3:7 EC/EMC, (b) 0.01 M $Li_2B_{12}H_3F_9$ and 1.0 M $LiPF_6$ in 3:7 EC/EMC, and (c) 0.01 M $Li_2B_{12}F_{12}$ and 1.0 M $LiPF_6$ in 3:7 EC/EMC. Measurements were done with a Pt/Li/Li three-electrode system.

Figure 3 shows cyclic voltammograms of 0.01 M $Li_2B_{12}F_{12}$ with different scanning rates. Again, the background solution is 1.0 M $LiPF_6$ in 3:7 EC/EMC. The curves show that the peak current (i_p) increases with the scanning rate. More specifically, Fig. 4a shows that the peak current increases linearly with the square root of the scanning rate ($\upsilon^{1/2}$), which is a typical characteristic of a diffusion-controlled interface electron transfer reaction. Also, both solutions with 0.01 M lithium borate cluster salts have the same peak current at various scanning rates, which indicates a similar diffusion coeffi-

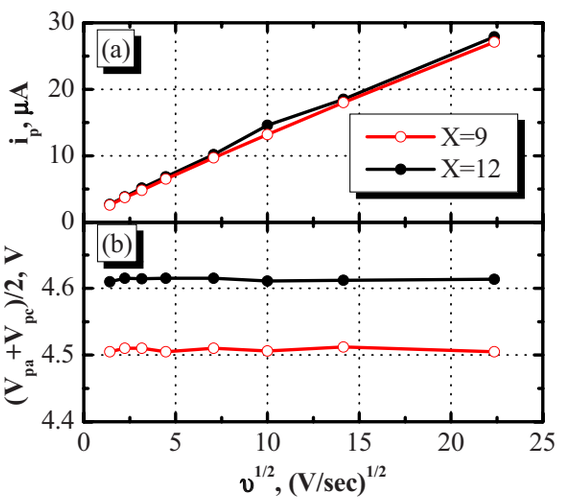

Figure 4. (Color online) Dependence of (a) peak current and (b) average peak potential on the scanning rate for 0.01 M $Li_2B_{12}H_3F_9$ and 0.01 M $Li_2B_{12}F_{12}$ in 1.0 M $LiPF_6$ in 3:7 EC/EMC.

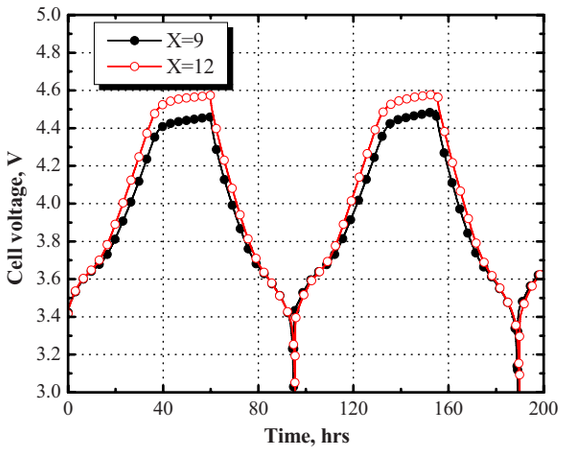

Figure 5. (Color online) Voltage profiles of two MCMB/$LiMn_{1/3}Ni_{1/3}Co_{1/3}O_2$ cells. Both cells were first charged for 60 h with a constant current of 0.1 mA and then discharged with a constant current of 0.1 mA. The electrolyte is 1.0 M $LiPF_6$ in 3:7 EC/dimethyl carbonate with the 0.08 M $Li_2B_{12}H_3F_9$ and 0.08 M $Li_2B_{12}F_{12}$ additives, respectively.

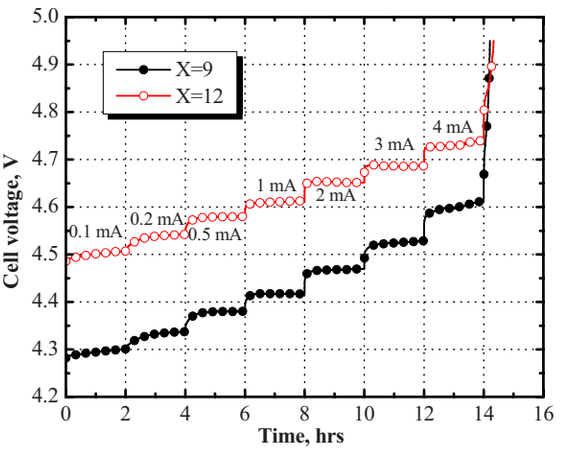

Figure 6. (Color online) Voltage of MCMB/$LiMn_{1/3}Ni_{1/3}Co_{1/3}O_2$ cells under stepwise overcharge with different applied currents. The electrolytes are 0.4 M $Li_2B_{12}H_3F_9$ and 0.4 M $Li_2B_{12}F_{12}$ in 3:7 EC/EMC.

cient in the electrolyte and a similar heterogeneous electron transfer constant for both anions, $B_{12}F_9H_3^{2-}$ and $B_{12}F_{12}^{2-}$. Equation 4 gives a theoretical description on the relationship between i_p and $v^{1/2}$

$$i_p = 2.69 \times 10^5 n^{3/2} A D^{1/2} v^{1/2} C \qquad [4]$$

where A is the surface area of the working electrode (cm^2), n is the number of electrons involved in the redox process ($n = 1$ for this case), C is the concentration of the active material in the solution (mol/cm^3), and D is the diffusion coefficient (cm^2/s). Based on Eq. 4, the diffusion coefficient for both anions is 2.1×10^{-6} cm^2/s.

Figure 3 also shows that with an increase in the scanning rate, the peak potential of the anionic reaction shifts to a higher potential, while the peak potential of the cathodic peak shifts to a lower potential. The shift in the peak potential with the scanning rate may be caused by the limited charge-transfer kinetics of the active species ($B_{12}H_xF_{12-x}^{2-}$) and the uncompensated resistance, which is commonly called the "IR drop." Because the polarization from the kinetic effect and IR drop is triggered by the current flowing through the electrochemical cell, the average peak potential $[(E_{pa} + E_{pc})/2]$ gives a fairly good estimation of the redox potential of the reversible electroactive species. Figure 4b shows that the average peak potentials of $B_{12}H_3F_9^{2-}$ and $B_{12}F_{12}^{2-}$ in EC:EMC (3:7) are about 4.5 and 4.6 V vs Li^+/Li, respectively.

Figure 5 shows the voltage profiles of two MCMB/L333 cells that were charged, overcharged, and discharged with a constant current of 0.1 mA. Both cells contained an electrolyte of 1.0 M $LiPF_6$ in 3:7 EC/EMC and 0.08 M of $Li_2B_{12}H_3F_9$ or $Li_2B_{12}F_{12}$ as the electrolyte additive. At the beginning, both cells were normally charged up to 40 h to deliver their full practical capacity. After that, both cells were further charged for another 20 h with the same current, in which step overcharge occurred, the potential of the positive electrode reached the redox potential of the anions, and the shuttle mechanism of the anions was activated. Figure 5 clearly shows 20 h long voltage plateaus at 4.4 and 4.55 V under the overcharge condition for $Li_2B_{12}H_3F_9$ and $Li_2B_{12}F_{12}$, respectively. The voltage plateaus are contributed by the shuttle mechanism of the borate cluster anions, which carry most of the current forced by the charger through the lithium-ion cells. However, because the concentration of the lithium borate cluster salts is very low (0.08 M), only a small limiting shuttle current is predicted according to Eq. 3, i.e., slightly smaller than 0.1 mA. Hence, a small portion of the overcharge current might not be completely handled by the borate cluster anions. This extra current can then slowly charge the lithium-ion cells and cause the slow voltage increase on the overcharge plateaus. This problem can be easily solved by increasing the concentration of the redox shuttle additives to provide a higher limiting shuttle current.

Figure 6 shows the dependence of the shuttle plateau voltage on the applied current for two MCMB/L333 cells. The electrolytes are 0.4 M $Li_2B_{12}H_3F_9$ and 0.4 M $Li_2B_{12}F_{12}$ in 3:7 EC/EMC. The current applied for each stage is labeled in Fig. 6. Clearly, the shuttle plateau voltage increases with the applied current. This figure also shows that the maximum shuttle current for both electrolytes is about 4 mA. It has also been reported that the shuttle current at different voltages can be fitted by the following equation[14]

$$V = V_0 + k \ln\frac{I}{I_{max} - I} + IR \qquad [5]$$

where R is the dc internal resistance of the cell, I_{max} is the limiting shuttle current, and k is a constant. The fitting results show that the maximum shuttle current for 0.4 M $Li_2B_{12}H_3F_9$ and 0.4 M $Li_2B_{12}F_{12}$ in EC:EMC (3:7) is 4.26 and 4.47 mA per 1.6 cm^2, respectively.

Conclusions

Two lithium borate cluster salts, $Li_2B_{12}H_3F_9$ and $Li_2B_{12}F_{12}$, were investigated as lithium salts and redox shuttles for the overcharge protection of lithium-ion cells. Due to the structural similarity between $B_{12}H_3F_9^{2-}$ and $B_{12}F_{12}^{2-}$, both salts possess very close chemical and physical properties in terms of conductivity, diffusion coefficient, heterogeneous charge-transfer constant, and maximum shuttle current; however, the redox potential of $B_{12}F_{12}^{2-}$ is about 0.1 V higher than that of $B_{12}H_3F_9^{2-}$. This class of lithium salts has two unique features that make them extremely promising for the overcharge protection of lithium-ion cells. First, their redox potential is tunable with the degree of fluorination. As a result, it is possible to design the redox shuttle for both different positive electrode materials and general applications. Second, their good solubility and capability of being the main salts in the electrolyte make them suitable for long-life and safe lithium-ion batteries.

Acknowledgment

Research funded by Air Products and Chemicals, Inc., Argonne National Laboratory is operated for the U.S. Department of Energy by UChicago Argonne, LLC, under contract DE-AC0Z-06CH11357.

Argonne National Laboratory assisted in meeting the publication costs of this article.

References

1. R. A. Leising, M. J. Palazzo, E. S. Takeuchi, and K. J. Takeuchi, *J. Electrochem. Soc.*, **148**, A838 (2001).
2. T. Ohsaki, T. Kishi, T. Kuboki, N. Takami, N. Shimura, Y. Sato, M. Sekino, and A. Satoh, *J. Power Sources*, **146**, 97 (2005).
3. R. A. Leising, M. J. Palazzo, E. S. Takeuchi, and K. J. Takeuchi, *J. Power Sources*, **97–98**, 681 (2001).
4. H. Wang and M.-C. Chen, *Electrochem. Solid-State Lett.*, **9**, A82 (2006).
5. K. M. Abraham, D. M. Pasquariello, and E. B. Willstaedt, *J. Electrochem. Soc.*, **137**, 1856 (1990).
6. M. N. Golovin, D. P. Wilkinson, J. T. Dudley, D. Holonko, and S. Woo, *J. Electrochem. Soc.*, **139**, 5 (1992).
7. M. Adachi, U.S. Pat. 5763119 (1998).
8. M. Adachi, K. Tanaka, and K. Sekai, *J. Electrochem. Soc.*, **146**, 1256 (1999).
9. D. Y. Lee, H. S. Lee, H. S. Kim, H. Y. Sun, and D. Y. Seung, *Korean J. Chem. Eng.*, **19**, 645 (2002).
10. X. M. Zhu, H. X. Yang, and X. P. Ai, *Electrochim. Acta*, **48**, 4033 (2003).
11. K. Amine, J. Liu, K. Jambunathan, B. K. Peterson, and G. Dantsin, U. S. Pat. Appl. 20050227143 (2005).
12. C. Buhrmester, J. Chen, L. Moshurchak, J. W. Jiang, R. L. Wang, and J. R. Dahn, *J. Electrochem. Soc.*, **152**, A2390 (2005).
13. J. Chen, C. Buhrmester, and J. R. Dahn, *Electrochem. Solid-State Lett.*, **8**, A59 (2005).
14. J. R. Dahn, J. W. Jiang, L. M. Moshurchak, M. D. Fleischauer, C. Buhrmester, and L. J. Krause, *J. Electrochem. Soc.*, **152**, A1283 (2005).
15. Z. H. Chen, Q. Z. Wang, and K. Amine, *J. Electrochem. Soc.*, **153**, A2215 (2006).
16. Z. H. Chen and K. Amine, *Electrochem. Commun.*, **9**, 703 (2007).
17. Z. H. Chen and K. Amine, *Electrochim. Acta*, **53**, 453 (2007).
18. S. R. Narayanan, S. Surampudi, A. I. Attia, and C. P. Bankston, *J. Electrochem. Soc.*, **138**, 2224 (1991).